# Stereological estimation of mean volume: precision of three simple sampling designs

**Kiên Kiêu**[1]

**Marianne Mora**

**Unité Mathématiques et Informatique Appliquées**
**INRA**
**Domaine de Vilvert**
**F-78352 Jouy-en-Josas Cedex**

[1] Kien.Kieu@jouy.inra.fr

**Abstract**

New approximation formulae for the mean square error of stereological volume predictors are derived. The body under investigation is assumed to be an isotropic random compact set. Three simple systematic sampling probes are considered: lattice of points, serial sections, clustered sections. The derived formulae depend only on the mean body surface area and sampling parameters. The key argument is a refined result on the convergence of the spectral density of compact sets.

# Stereological estimation of mean volume: precision of three simple sampling designs

## 1 Introduction

Stereology is the inference of spatial structures from partial observations performed on lower-dimensional probes, typically thin of thick sections. Stereological methods are commonly used in order to determine geometric characteristics of bodies such as volume or surface area.

Standard stereological estimators are sums of measurements performed on sampling probes, e.g. areas measured on sections. These estimators are unbiased for a wide class of spatial structures provided that the probes sample uniformly the containing space. Assessing mean square error is not a trivial task because of likely correlations between measurements on neighbour probes.

Kendall [9] considered a very simple stereological method (planar area estimation based on counts on a point grid) and derived an expression of the mean square error based on the power spectral density of the planar body under investigation. The power spectral density (PSD) of a body is defined as the squared modulus of its indicator function. Using the method of the stationary phase, Kendall obtained an asymptotic approximation of the PSD in terms of features of the body boundary. A mean square error approximation based on the PSD approximation was proposed. This approximation can be decomposed into two terms of the same order: a central term and an oscillating term.

Kendall's approach has been generalised by Matheron [12], [13], [14] for spatial structures in spaces with arbitrary dimensions to the estimation of other geometric parameters and to other sampling schemes. Furthermore Matheron proposed to ignore the oscillating term of the mean square error. This term is difficult to estimate from available data. Also empirical studies tend to show that the oscillating term is small compared to the central term (named extension term by Matheron).

Matheron's methods also called transitive methods are used to assess the precision of commonly used stereological estimators, see e.g. [6, 4].

In a recent paper [11], we have considered a stochastic approach where the body under investigation is assumed to be random. In such a framework asymptotics for the PSD are easier to derive. Moreover the MSE approximations derived from the PSD asymptotics only involve the extension term: in this stochastic framework the oscillating term turns

out to be of higher-order compared the extension term. This stochastic framework is quite natural in many biological studies where the body under investigation is subject to biological variability.

Note that since the body under investigation is assumed to be random, its volume is now a random variable. Therefore the stereological procedures used to evaluate the volume may be considered as predictors rather than estimators.

The aim of this paper is to derive MSE formulae for stereological predictors based on other sampling probes than point grids. The key point is a very simple relationship derived by Matheron between the PSD of point-wise measurements (i.e. hits) and the PSD of higher-dimensional measurements (e.g. areas measured on sections).

We focus on volume prediction and three particular common sampling schemes: lattice of points, series of sections and series of clustered sections. For sake of simplicity, the random body is assumed to be isotropic.

Section 2 is devoted to the general framework of the present paper. The random body is set up as a random compact shape subjected to the action of a particular group of geometrical transformations. Within this framework, we state the regularity conditions under which the asymptotic approximation formula of the spectral density is obtained. Sections 3 and 4 are concerned with the three stereological sampling schemes: lattice of points, series of sections and series of clustered sections. In each case, we introduce the sampling scheme and the related stereological volume predictor. The mean square error is expressed in terms of the spectral density of the random body and an asymptotic formula is given. These formulae involve the mean surface area of the random body. In Section 5 we compare the precision of the different sampling designs. Concluding remarks are given in Section 6.

## 2   General framework

### 2.1   Spectral density of a random body

Let $\mathcal{K}$ denote the space of bodies (compacts sets) in $\mathbb{R}^3$ endowed with the hitting topology (see e.g. [15]).

Let us consider a random body $\mathbf{X}$ in $\mathbb{R}^3$, see Figure **1**. We shall denote by $\mathbf{V}$ and $V$ the volume and mean volume of $\mathbf{X}$ and by $\mathbf{S}$ and $S$ the boundary area and mean boundary area of $\mathbf{X}$ respectively.

The spectral density $\mathrm{PSD}_{\mathbf{X}}$ of a random body $\mathbf{X}$ is defined as the mean squared modulus of the Fourier transform of the indicator function $I_{\mathbf{X}}$ of the random body, i.e.

$$\mathrm{PSD}_{\mathbf{X}}(y) = \mathrm{E}\left[\left|\int_{\mathbb{R}^3} I_{\mathbf{X}}(x)\exp\left(-2\pi i x \cdot y\right)\,dx\right|^2\right], \quad y \in \mathbb{R}^3. \tag{1}$$

Note that the spectral density is also the Fourier transform of the (geometric) covariogram of the random body $\mathbf{X}$ defined as the mean of the convolution product $I_{\mathbf{X}} * I_{-\mathbf{X}}$ where $I_{\mathbf{X}}$ is the indicator function of $\mathbf{X}$.
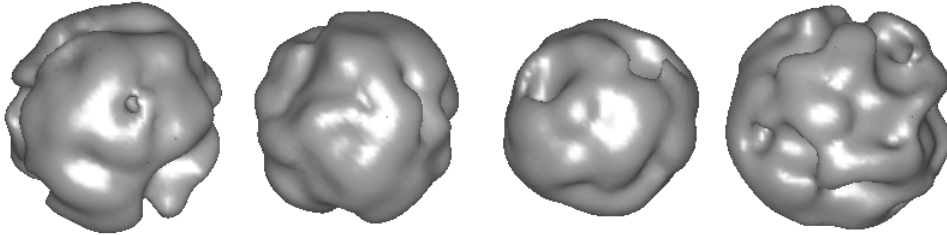
Figure 1: Four realisations of an isotropic random body.

## 2.2 Asymptotic formula of the spectral density

We are concerned with the asymptotic behaviour of the spectral density

$$\text{PSD}_{\mathbf{X}}\left(\rho\omega_0\right), \quad \omega_0 \in \Omega, \rho \to \infty.$$

Here $\Omega$ denotes the unit sphere.

Below, we state a general convergence result for the spectral density of a random body $\mathbf{X}$ as defined in formula (5). This convergence result involves the mean boundary area $S$ and the rose of unoriented normal directions to the boundary $\partial\mathbf{X}$ of $\mathbf{X}$, see e.g. [16]. The rose can be considered as a probability measure on the unit hemisphere. We shall assume that rose of normal directions admits a density function $r$.

Under regularity conditions listed in the next section, the asymptotic formula of the spectral density is the following:

$$\lim_{\rho \to \infty} \rho^4 \, \text{PSD}_{\mathbf{X}}\left(\rho\omega_0\right) = \frac{S \, r\left(\omega_0\right)}{4\pi^2}. \tag{2}$$

The asymptotic result (2) is supplemented by the following estimate:

$$\sup_{\rho,\omega_0} \rho^4 \, \text{PSD}_{\mathbf{X}}\left(\rho\omega_0\right) < \infty. \tag{3}$$

For sake of simplicity, we shall restrict our statistical study (sections 3 and 4) to a random body $\mathbf{X}$ which distribution is invariant by orthogonal transformations. In particular, $\mathbf{X}$ is assumed to be isotropic. In this particular case, the normal directions to the boundary of $\mathbf{X}$ are uniformly distributed on the hemisphere. Hence, the approximation formula of the spectral density becomes

$$\lim_{\rho \to \infty} \rho^4 \, \text{PSD}_{\mathbf{X}}\left(\rho\omega_0\right) = \frac{S}{8\pi^3}. \tag{4}$$
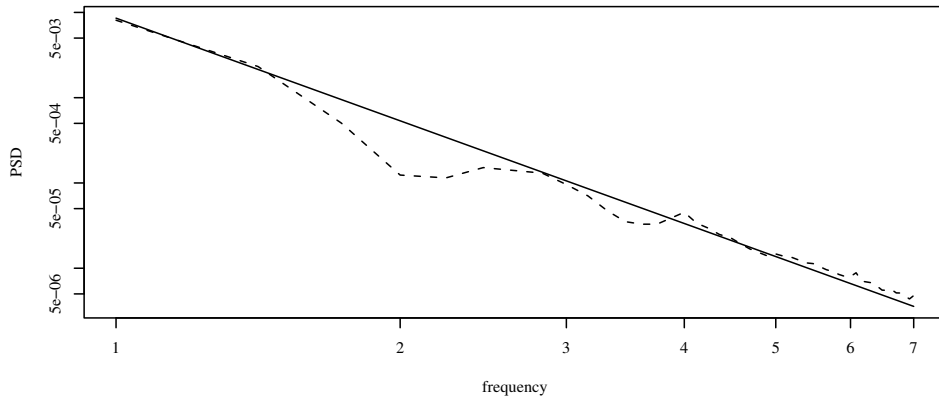
3

Figure 2: Spectral density of a random body and its asymptotic approximation. The spectral density (dashed line) is computed from 200 realisations of the random body. The realisations are obtained by the simulation procedure used in Figure 1. The asymptotic approximation (solid line) is computed from Formula (2).

## 2.3   Regularity conditions

The asymptotic results provided in Section 2.2 hold under some regularity conditions. Following [11], the regularity conditions involve the conditional distribution of the size and the orientation of the random body $\mathbf{X}$ given its shape.

Under the action of translations, orthogonal transformations and dilatations, the space of bodies can be decomposed into orbits. Each orbit defines a shape and can be assigned a representative. Hence a random body $\mathbf{X}$ can be decomposed into

$$\mathbf{X} = \mathbf{hPF} + \mathbf{v}, \tag{5}$$

where $\mathbf{h}$ is a random dilatation factor, $\mathbf{P}$ is a random orthogonal transformation, $\mathbf{F}$ is a random (representative) shape and $\mathbf{v}$ is a random translation vector.

The asymptotic results given in Section 2.2 hold if

**Condition 1** The random body $\mathbf{X}$ is a.s. uniformly bounded in $\mathbb{R}^3$.

**Condition 2** The boundary $\partial\mathbf{X}$ of $\mathbf{X}$ is a.s. a compact $C^1$-manifold and the mean boundary area $S$ of $\mathbf{X}$ is finite.

**Condition 3** The conditional distribution of $(\mathbf{h}, \mathbf{P})$ given $\mathbf{F}$ has a continuous and uniformly bounded (w.r.t. $\mathbf{F}$) density with respect to the product of the Lebesgue measure on $\mathbb{R}_+$ and the Haar probability measure on the group of orthogonal transformations.

4

In the degenerated case where $\mathbf{X}$ is deterministic, the convergence results (2) and (3) do not hold. However a convergence result similar to Formula (2) can be derived using the method of the stationary phase, see e.g. [8]. Then the limit involves an extra term which can be written as a sum of oscillating functions. Each of these functions is associated with a pair of points on the boundary of the body where both normals are parallel to $\omega_0$.

From now on, we shall assume that the random body $\mathbf{X}$ is isotropic and fulfils Conditions 1–3.

# 3   Point sampling design

We consider a random body $\mathbf{X}$ with volume $\mathbf{V}$. The problem considered here is to predict $\mathbf{V}$ from measurements on the intersection of $\mathbf{X}$ with random sampling probes. The volume predictor depends on the dimension of the sampling probes. In the case where $\mathbf{X}$ is sampled by a lattice of points, the volume prediction is based on the number of points hitting the body.

## 3.1   Volume stereological predictor

We consider a three-dimensional lattice of points $\Lambda_1$ in $\mathbb{R}^3$ defined by

$$\Lambda_1 = \left\{ Ek : k \in \mathbb{Z}^3 \right\}, \tag{6}$$

where the generator matrix $E$ is a $3 \times 3$ non singular real matrix. We denote $\lambda$ the determinant of $E$. Note that $\lambda$ is the volume of the fundamental tile of the lattice.

In order to get a lattice with uniform random location, $\Lambda_1$ is translated by $E\mathbf{U}$ where $\mathbf{U}$ is a uniform random point in the cube $[0,1]^3$. Then $X$ is sampled by the random lattice $\mathbf{\Lambda}_1$ defined by

$$\mathbf{\Lambda}_1 = \Lambda_1 + E\mathbf{U},$$

see Figure 3. Notice that the distribution of $\mathbf{\Lambda}_1$ is invariant under translation.

The volume predictor $\widehat{\mathbf{V}}_1$ associated with this sampling design is defined by

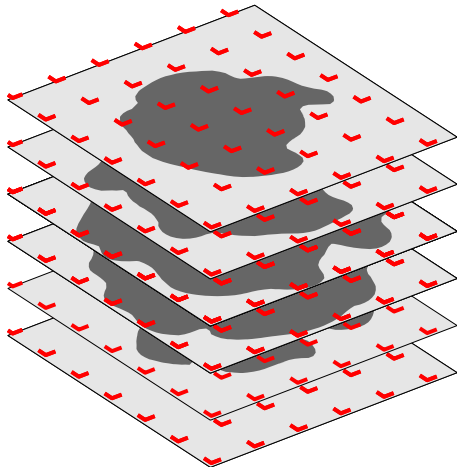$$\widehat{\mathbf{V}}_1 = \lambda \sum_{x \in \mathbf{\Lambda}_1} I_{\mathbf{X}}(x). \tag{7}$$

Since the distribution of $\mathbf{\Lambda_1}$ is invariant under translation, one has

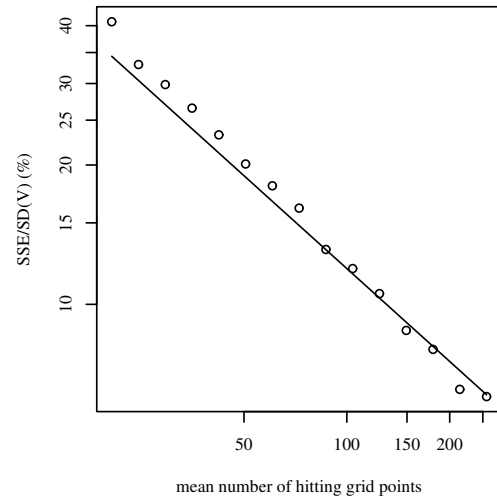$$\mathrm{E}\left[\widehat{\mathbf{V}}_1 \mid \mathbf{X}\right] = \mathbf{V}.$$

## 3.2   Mean square stereological error

The precision of the predictor $\widehat{\mathbf{V}}_1$ can be assessed from the mean square stereological error (MSSE) defined as

$$\mathrm{MSSE}\left[\widehat{\mathbf{V}}_1\right] = \mathrm{E}\left[\left(\widehat{\mathbf{V}}_1 - \mathbf{V}\right)^2\right].$$

(a) Body sampled by a grid of points

(b) SSE approximation

Figure 3: Volume prediction and point sampling design. Right (b): the ratio between the standard stereological error SSE ($MSSE = SSE^2$) and the volume standard deviation is plotted for various grid densities. The standard stereological error (circles) is computed by simulating twice the sampling of 200 bodies. The standard stereological error approximation (solid line) is computed from Formula (10).

The mean square stereological error of $\widehat{\mathbf{V}}_1$ can be expressed in terms of the spectral density of $\mathbf{X}$. This type of result has been proved by Kendall [9] in a deterministic framework. Conditionally on $\mathbf{X}$ the predictor $\widehat{\mathbf{V}}_1$ can be considered as a periodic function of the random shift $\mathbf{U}$. Using Parseval equality and simple Fourier calculus, it is easily shown that

$$\text{MSSE}\left[\widehat{\mathbf{V}}_1\right] = \sum_{y \in \Lambda_1^* \setminus \{0\}} \text{PSD}_{\mathbf{X}}(y), \tag{8}$$

where $\Lambda_1^*$ is the dual lattice of $\Lambda_1$ with generator matrix $E^* = \left(E^{-1}\right)'$.

## 3.3   Approximation formula

We are interested in the asymptotic behaviour of the mean square stereological error for dense systematic sampling probes, i.e. for small values of $\lambda$. Introducing the "unit" three-dimensional lattice $\Lambda = \lambda^{-\frac{1}{3}} \Lambda_1$, the mean square stereological error can be written as

$$\text{MSSE}\left[\widehat{\mathbf{V}}_1\right] = \sum_{y \in \Lambda^* \setminus \{0\}} \text{PSD}_{\mathbf{X}}\left(\lambda^{-\frac{1}{3}} y\right).$$

For each $y \in \Lambda^*$, Formulae (4) and (3) applied with $\rho = \lambda^{-\frac{1}{3}} \|y\|$ yield the limit

$$\lim_{\lambda \to 0} \lambda^{-\frac{4}{3}} \text{PSD}_{\mathbf{X}}\left(\lambda^{-\frac{1}{3}} y\right) = \|y\|^{-4} \, \frac{S}{8\pi^3}$$

together with the inequality

$$\lambda^{-\frac{4}{3}} \text{PSD}_{\mathbf{X}}\left(\lambda^{-\frac{1}{3}} y\right) \le \|y\|^{-4} \, C, \quad C < \infty.$$

Hence the approximation formula for the mean square stereological error is

$$\text{MSSE}\left[\widehat{\mathbf{V}}_1\right] \sim \lambda^{\frac{4}{3}} \frac{S}{8\pi^3} \sum_{y \in \Lambda^* \setminus \{0\}} \|y\|^{-4}, \quad \lambda \to 0.$$

Introducing the Epstein zeta function $Z_{\Lambda^*}$ associated with the lattice $\Lambda^*$ of points in $\mathbb{R}^3$ and defined by

$$Z_{\Lambda^*}(s) = \sum_{y \in \Lambda^* \setminus \{0\}} \|y\|^{-s}, \quad s > 3, \tag{9}$$

one finally gets

$$\text{MSSE}\left[\widehat{\mathbf{V}}_1\right] \sim \lambda^{\frac{4}{3}} \frac{S}{8\pi^3} Z_{\Lambda^*}(4), \quad \lambda \to 0. \tag{10}$$

Note that the limit above is the extension term obtained by Matheron [12] in a deterministic framework. Matheron's formula is based on a numerical approximation of the Epstein zeta function. See Section 5 for more details.

A comparison between simulated and approximated mean square stereological errors is provided in Figure 3.

7

# 4 Serial and clustered section sampling designs

These two sampling designs involve a series of parallel planes intersecting the body $\mathbf{X}$. In this case, the mean volume can be predicted from profile areas measured on the sampling sections.

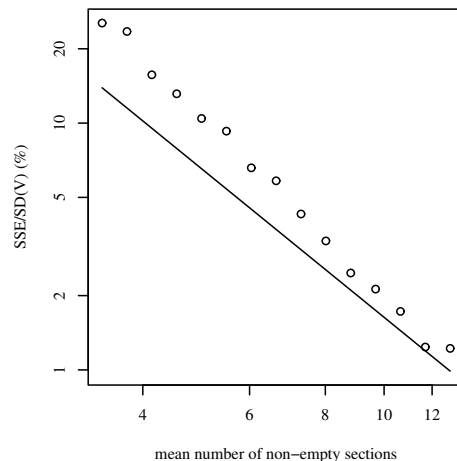## 4.1 Serial section sampling design

Here the body is intersected by parallel equidistant planes, see Figure 4. The orientation of the planes is considered as fixed. Without loss of generality, we may assume that the planes are horizontal. Any horizontal plane can be identified to its intersection with the vertical axis. Thus parallel equidistant planes are identified to a one-dimensional vertical lattice of points. The series of planes is said to be uniform random if the one-dimensional lattice of points can be written as

$$\mathbf{\Lambda}_2 = \left\{ (k + \mathbf{U})\,\delta\omega : k \in \mathbb{Z} \right\}, \tag{11}$$

where $\mathbf{U}$ is uniformly distributed in $[0, 1]$, $\delta$ is the distance between two neighbour planes and $\omega$ is a unit vertical vector in $\mathbb{R}^3$.
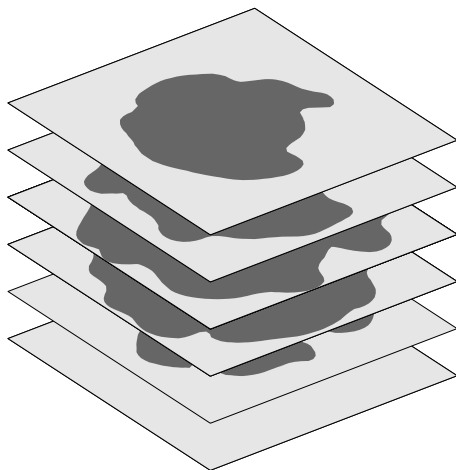


(a) Serial sections

(b) SSE approximation

Figure 4: Volume prediction and serial section sampling design. Right (b): the ratio between the standard stereological error SSE and the volume standard deviation is plotted for various sampling densities. The standard stereological error (circles) is computed by simulating twice the sampling of 200 bodies. The standard stereological error approximation (solid line) is computed from Formula (15).

8

The unbiased volume predictor associated with this sampling probe, so-called Cavalieri predictor (when the body under investigation is deterministic), is

$$\widehat{\mathbf{V}}_2 = \delta \sum_{x \in \mathbf{\Lambda}_2} \mathbf{A}(x) \tag{12}$$

where $\mathbf{A}(x)$ denotes the area of $\mathbf{X}$ measured on the sampling section hitting the vertical axis at point $x$. Using the same arguments as for Equation (8), it can be shown that

$$\mathrm{MSSE}\left[\widehat{\mathbf{V}}_2\right] = \sum_{k \in \mathbb{Z} \setminus \{0\}} \mathrm{PSD}_{\mathbf{A}}\left(\frac{k}{\delta}\omega\right),$$

where $\mathrm{PSD}_{\mathbf{A}}$ is defined as the mean squared modulus of the Fourier transform of the function $\mathbf{A}$ considered as a function on the vertical axis.

The profile area function $\mathbf{A}$ in (12) is obtained by integrating $I_{\mathbf{X}}$ over horizontal planes. This integration operation is called *grading* by Matheron [12, 14]. Using Matheron's general result on the spectral density of a graded regionalized variable, one gets

$$\mathrm{PSD}_{\mathbf{A}}(y) = \mathrm{PSD}_{\mathbf{X}}(y), \tag{13}$$

for any $y$ on the vertical axis. This relationship is a straightforward consequence of the fact that the Fourier transform of the area measure on the horizontal plane through the origin is just the length measure on the vertical axis.

Using (13), we can then express the mean square stereological error as

$$\mathrm{MSSE}\left[\widehat{\mathbf{V}}_2\right] = \sum_{k \in \mathbb{Z} \setminus \{0\}} \mathrm{PSD}_{\mathbf{X}}\left(\frac{k}{\delta}\omega\right). \tag{14}$$

We will give now an approximation formula for the mean square stereological error when the spacing $\delta$ between section planes tends to 0.

For each $k \in \mathbb{Z}$, Formulae (4) and (3) applied with $\rho = k/\delta$ yield the limit

$$\lim_{\delta \to 0} \delta^{-4} \mathrm{PSD}_{\mathbf{X}}\left(\frac{k}{\delta}\omega\right) = k^{-4}\frac{S}{8\pi^3}$$

with the inequality

$$\delta^{-4} \mathrm{PSD}_{\mathbf{X}}\left(\frac{k}{\delta}\omega\right) \le k^{-4}C, \quad C < \infty.$$

The approximation formula for the mean square stereological error is then

$$\mathrm{MSSE}\left[\widehat{\mathbf{V}}_2\right] \sim \frac{S}{8\pi^3}\delta^4 \sum_{k \in \mathbb{Z} \setminus \{0\}} k^{-4}, \quad \delta \to 0.$$

The infinite sum is equal to $2\zeta(4)$ where $\zeta$ denotes the zeta function, and simplifies as $\pi^4/45$. One finally gets

$$\mathrm{MSSE}\left[\widehat{\mathbf{V}}_2\right] \sim \frac{S\pi}{360}\delta^4, \quad \delta \to 0. \tag{15}$$

The precision of the Cavalieri predictor has been investigated in previous papers. In particular, it has been shown that when $X$ is a deterministic ellipsoid (fixed size and orientation) the mean square stereological error tends to 0 as fast as $\delta^4$, see [3]. In [6] general mean square stereological error approximations have been derived using the transitive methods. Due to a misinterpretation of Matheron's theory it has been stated that the mean square stereological error of the Cavalieri predictor tends to 0 as fast as $\delta^2$. In [5], the application of the transitive methods has been reconsidered and it has been stated that for "quasi-ellipsoidal bodies" the variance of the Cavalieri predictor tends to 0 as fast as $\delta^4$. This statement has been further investigated in [10, 7] where the result is extended to bodies with curved boundaries.

Note that the variance approximations derived in [5, 10, 7] are of the type $C\delta^4$ where $C$ is not given a geometric interpretation. Instead $C$ is expressed as a covariogram derivative at the origin.

A comparison between simulated and approximated mean square stereological errors is provided in Figure 4.

## 4.2   Clustered section sampling design

Next let us consider a sampling scheme where the section planes are distributed as a series of clusters, see Figure 5. This type of sampling scheme can be practically implemented through a two-stage procedure:

- First the spatial structure under investigation is sliced into physical slabs.

- Then a sample of slabs (e.g. every tenth slab) are investigated by means of (optical) sections.

As in Section 4, the section planes are assumed to be horizontal and any section plane is identified with its intersection with the vertical axis. The section planes are randomised such that the series of points on the vertical axis can be written as

$$\mathbf{\Lambda}_3 = \left\{ \left( \left( k + \mathbf{U} \right) \Delta + l\delta \right) \omega : k \in \mathbb{Z}, l = 1, \ldots, m \right\},$$

where $\mathbf{U}$ is uniformly distributed in $[0, 1]$, $\Delta$ is the distance between the "first" section planes of neighbour clusters, $\delta$ is the distance between neighbour section planes within a cluster and $m$ is the number of section planes per cluster.

The volume predictor associated with this sampling scheme is

$$\widehat{\mathbf{V}}_3 = \frac{\Delta}{m}\delta \sum_{x \in \mathbf{\Lambda}_3} \mathbf{A}\left( x \right). \tag{16}$$

Note that when $\Delta = m\delta$, the section planes the total sampling fraction is equal to 1 and the series $\mathbf{\Lambda}_3$ defines an ordinary series of sections with spacing equal to $\Delta/m$.
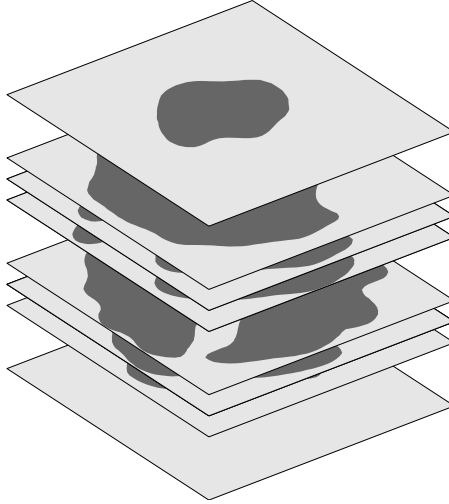
Figure 5: Volume prediction and clustered section sampling design.

The mean square stereological error of $\widehat{\mathbf{V}}_3$ is given by

$$\text{MSSE}\left[\widehat{\mathbf{V}}_3\right] = \frac{\delta^2}{t^2} \sum_{k \in \mathbb{Z} \setminus \{0\}} \text{PSD}_{\mathbf{X}}\left(\frac{k}{\Delta}\omega\right) \sum_{l_1, l_2 = 1}^{m} \exp\left(\frac{2\pi i \left(l_1 - l_2\right) k\delta}{\Delta}\right). \qquad (17)$$

This formula is derived by using the same technical approach as before. First the mean square stereological error can be written as

$$\text{MSSE}\left[\widehat{\mathbf{V}}_3\right] = \frac{\delta^2}{t^2} \sum_{k \in \mathbb{Z} \setminus \{0\}} \text{PSD}_{\mathbf{A} * T_m}\left(\frac{k}{\Delta}\omega\right)$$

where $T_m$ denotes the finite sum of Dirac measures at $\delta\omega, 2\delta\omega, ..., m\delta\omega$. Note that the convolution product $\mathbf{A} * T_m\left(x\right)$ is the sum of section areas measured inside the slab associated with $x$.

The spectral density of the convolution product is just the product of the spectral density of $\mathbf{A}$ with the spectral density of $T_m$. The square modulus of the Fourier transform of $T_m$ is given by

$$\text{PSD}_{T_m}\left(y\right) = \sum_{l_1, l_2 = 1}^{m} \exp\left(2\pi i \left(l_1 - l_2\right) \delta\omega \cdot y\right).$$

Combining this result together with Formula (13), one gets the mean square stereological error formula (17).

We are concerned with the asymptotic behaviour of the mean square stereological error for small values of $\Delta$. For $\Delta$ tending to 0, the approximation formula for the mean square

11

stereological error is

$$\mathrm{MSSE}\left[\widehat{\mathbf{V}}_3\right] \sim \frac{S\,\pi}{12}\frac{\delta^2}{t^2}\Delta^4\left(\frac{m^2}{30} - 2\sum_{l=1}^{m}(m-l)\left(\frac{l\delta}{\Delta}\right)^2\left(\frac{l\delta}{\Delta}-1\right)^2\right). \qquad (18)$$

To obtain this asymptotic formula, we first apply Formulae (4) and (3) to (17). This yields the limit result

$$\lim_{\Delta\to 0}\Delta^{-4}\,\mathrm{MSSE}\left[\widehat{\mathbf{V}}_3\right] = \frac{S}{8\pi^3}\frac{\delta^2}{t^2}\sum_{l_1,l_2=1}^{m}\sum_{k=1}^{\infty}k^{-4}\exp\left(\frac{2\pi i\,(l_1-l_2)\,k\delta}{\Delta}\right).$$

Introducing the Bernoulli polynomial $B_4$ of index 4, the last result can be written as

$$\lim_{\Delta\to 0}\Delta^{-4}\,\mathrm{MSSE}\left[\widehat{\mathbf{V}}_3\right] = \frac{S\,\pi}{12}\frac{\delta^2}{t^2}\left(-mB_4\left(0\right) - 2\sum_{l=1}^{m}(m-l)\,B_4\left(\frac{l\delta}{\Delta}\right)\right).$$

The approximation formula (18) follows from using the polynomial expression of $B_4$.

Expanding the sum and using $f$, $t$ and $m$ as sampling parameters, one gets the alternative formula

$$\mathrm{MSSE}\left[\widehat{\mathbf{V}}_3\right]$$
$$\sim \frac{S\,\pi}{360}\frac{t^4}{f^4 m^4}\left(m^4\left(1+2f-2f^2\right)\left(1-f\right)^2 + 5m^2 f^2\left(1-f\right)^2 + f^3\left(4-3f\right)\right). \qquad (19)$$

This asymptotic approximation formula holds for fixed parameters $f$ and $m$ and slab thickness $t\to 0$.

Note that when all slabs are analysed ($f = 1$), Formula (19) reduces to the approximation formula (15) for sampling by serial sections with spacing $\delta = t/m$.

A comparison between exact and approximated mean square stereological errors is provided in Figure 5.

## 5    Comparisons of the sampling designs

The approximation formula (10) can be used in order to compare sampling point grids according to their shape (the sampling density being fixed i.e. $\lambda = 1$). Note that the Epstein zeta function $Z_{\Lambda^*}(4)$ can be computed numerically using the Chowla-Selberg expansion, see [2]. Matheron's approximation formula [12, page 105] is obtained from the first three terms of the Chowla-Selberg expansion. These first three terms depend only on particular values of the Riemann zeta function and on some Bernoulli numbers. Thus they are easily computed from numerical tables. Higher-order expansions used below involve values of Bessel functions.

When $\Lambda$ is the unit self-dual cubic lattice then

$$Z_{\Lambda^*}(4) = 16.53.$$

Next let us consider rectangular sampling lattices of the type $\Lambda = \alpha^{-\frac{1}{3}}\mathbb{Z} \times \alpha^{-\frac{1}{3}}\mathbb{Z} \times \alpha^{\frac{2}{3}}\mathbb{Z}$. When $\alpha > 1$, the horizontal density is higher than the vertical density. Numerical computations yield

| $\alpha:$ | 1 | 2 | 3 | 4 | 5 | 6 | 7 | 8 | 9 | 10 |
|---|---|---|---|---|---|---|---|---|---|---|
| $Z_{\Lambda^*}(4):$ | 16.53 | 25.01 | 50.36 | 96.21 | 166.5 | 265.1 | 395.6 | 561.2 | 765.5 | 1011 |

Hence under the isotropy assumption, the cubic sampling grid yields a better volume predictor than anisotropic rectangular sampling grids.

Better predictors are obtained using the centred cubic lattice or the face-centred cubic lattice: $Z_{\Lambda^*}(4) = 15.96$ and $Z_{\Lambda^*}(4) = 15.97$ respectively. In [1], it is shown that 16.96 is a local minimum for the function

$$\Lambda \rightarrow Z_{\Lambda^*}(4)$$

defined for all unit lattices $(\lambda = 1)$.

Based on the MSSE approximations formulae, the three predictors $\widehat{\mathbf{V}}_1$, $\widehat{\mathbf{V}}_2$ and $\widehat{\mathbf{V}}_3$ can be compared independently of the spatial structure under investigation.

First let us compare point and serial section sampling designs. These sampling designs are based respectively on a three-dimensional lattice of points $\Lambda_1$ and a vertical one-dimensional lattice of points $\Lambda_2$. For sake of simplicity, we take a rectangular lattice of points

$$\Lambda_1 = \delta \left( \alpha^{-1}\mathbb{Z}^2 \times \mathbb{Z} \right).$$

We consider the case where the vertical inter-distances $(\delta)$ of $\Lambda_1$ and $\Lambda_2$ are equal. Using approximations (10) and (15), for small values of $\delta$ we get

$$r_{12} = \frac{\mathrm{SSE}\left[\widehat{\mathbf{V}}_1\right]}{\mathrm{SSE}\left[\widehat{\mathbf{V}}_2\right]} \sim \sqrt{\frac{Z_{(\alpha\mathbb{Z}^2)\times\mathbb{Z}}(4)}{2\zeta(4)}}.$$

Below, we give numerical values of the ratio $r_{12}$ for some values of $\alpha$:

| $\alpha:$ | 1 | 2 | 3 |
|---|---|---|---|
| $r_{12}:$ | 2.8 | 1.3 | 1.1 |

Now let us compare serial and clustered section sampling designs. Consider the case where the mean number of sections hitting the body is the same for both sampling schemes: $\delta_1 = \delta_2/f$ where $\delta_1$ is the spacing for the serial sections and $\delta_2$ is the distance between two neighbour sections within a cluster. Using approximations (15) and (19), we get

$$r_{32} = \frac{\mathrm{SSE}\left[\widehat{\mathbf{V}}_3\right]}{\mathrm{SSE}\left[\widehat{\mathbf{V}}_2\right]} \sim \sqrt{1 + (1-f^2)(m-1)(m+1)(m^2 + 2m^2f - 2m^2f^2 + 3f^2 + 2f + 1)}.$$

The parameters $f$ and $m$ describe the type of clusters: $m$ is the cluster size and $f$ the cluster coverage fraction. When $m = 1$ or $f = 1$, both sampling schemes are equivalent.

Below the ratio $r_{32}$ of approximated standard stereological errors is computed for several cluster sizes $m$ and cluster coverage fractions $f$:

$$
\begin{array}{rcccc}
m: & 3 & 3 & 4 & 4 \\
f: & 0.1 & 0.5 & 0.1 & 0.5 \\
r_{32}: & 8.82 & 5.79 & 16.7 & 10.1
\end{array}
$$

# 6   Concluding remarks

In practice the mean boundary area $S$ is not known a priori and an estimation method is required. When the body $\mathbf{X}$ is intersected by a series of parallel sections, the mean surface area $S$ can be estimated from perimeters measured on sections. Standard estimation formulae can be found in [16] and [17].

For sake of simplicity we have focused on the case of an isotropic random body. Note that approximation formulae (15) and (19) can easily be extended to the anisotropic case. One just has to replace the mean surface area $S$ by $S\,r\,(\omega)$ where $\omega$ is the unit vector perpendicular to the section planes. The comparison ratio $r_{32}$ as given in Section 5 remains valid.

Some sampling designs used in microscopy are more complicated than those considered here. Approximations of the mean square stereological errors of these sampling designs are still required.

# Bibliography

[1] CHIU, P. (1997). Height of flat tori. *Proceedings of the American Mathematical Society* **125,** 723–730.

[2] CHOWLA, S. AND SELBERG, A. (1949). On Epstein's zeta function (I). *Proc. Acad. Sci. U.S.A.* **35,** 371–374.

[3] CRUZ-ORIVE, L. M. (1987). Precision of stereological estimators from systematic probes. *Acta Stereol.* **3,** 153–158.

[4] CRUZ-ORIVE, L. M. (1989). On the precision of systematic sampling: a review of Matheron's transitive methods. *J. Miscrosc.* **153,** 315–333.

[5] CRUZ-ORIVE, L. M. (1993). Systematic sampling in stereology. In *Proceedings of the 49th Session of the International Statistical Institute.* vol. 2. pp. 451–468.

[6] GUNDERSEN, H. J. G. AND JENSEN, E. B. (1987). The efficiency of systematic sampling in stereology and its prediction. *J. Miscrosc.* **147,** 229–263.

[7] GUNDERSEN, H. J. G., JENSEN, E. V., KIÊU, K. AND NIELSEN, J. (1999). The efficiency of systematic sampling in stereology and its prediction - reconsidered. *J. Miscrosc.* **193,** 199–211.

[8] HÖRMANDER, L. (1983). *The Analysis of Linear Partial Differential Operators I.* Springer-Verlag, Berlin.

[9] KENDALL, D. (1948). On the number of points of a given lattice inside a random oval. *Quart. J. Math. Oxford* **19,** 1–26.

[10] KIÊU, K., SOUCHET, S. AND ISTAS, J. (1999). Precision of systematic sampling and transitive methods. *J. Statist. Plan. Infer.* **77,** 263–279.

[11] KIÊU, K. AND MORA, M. (2004). Asymptotics for geometric spectral densities and a stochastic approach of the lattice-point problem. *Mathematicae Notae* **Año XLII,** 77–93.

[12] MATHERON, G. (1965). *Les variables régionalisées et leur estimation.* Masson, Paris.

[13] MATHERON, G. (1970). La théorie des variables régionalisées et ses applications. Les Cahiers du Centre de Morphologie Mathématique de Fontainebleau 5. École Nationale Supérieure des Mines de Paris.

[14] MATHERON, G. (1970). The theory of regionalized variables and its applications. Les Cahiers du Centre de Morphologie Mathématique de Fontainebleau 5bis. École Nationale Supérieure des Mines de Paris.

[15] MATHERON, G. (1975). *Random Sets and Integral Geometry.* Wiley series in probability and mathematical statistics. John Wiley & Sons, New-York.

[16] STOYAN, D., KENDALL, W. S. AND MECKE, J. (1987). *Stochastic Geometry and its Applications.* Wiley, Chichester.

[17] WEIBEL, E. R. (1980). *Stereological Methods. Vol. 2. Theoretical Fundations.* Academic Press.